VARIATIONS OF SOME SOLAR ACTIVITY INDICES AND MAGNETIC FIELDS OF CORONAL HOLES OF CYCLE 25

© 2025 O. A. Andreeva[a, **], E. A. Illarionov[b, **]

[a]*Crimean Astrophysical Observatory RAS (CrAO RAS), Nauchny, Russia*

[b]*Moscow State University (MSU), Moscow, Russia*

**e-mail: olga@craocrimea.ru*

***e-mail: egor.mypost@gmail.com*

Received March 11, 2025

Revised April 16, 2025

Accepted May 22, 2025

Abstract. The variations of sunspot indices and areas, as well as the areas and magnetic fluxes of coronal holes in the first five years of cycle 25 are considered. The source of initial data for analyses of sunspot indices and areas, as well as coronal hole areas, is https://observethesun.com. The magnetic fluxes of coronal holes were calculated from synoptic maps of magnetic fields obtained from observations of two independent instruments: the Helioseismic and Magnetic Imager/Solar Dynamics (HMI/SDO) and the Solar Operational Prediction Telescope/Kislovodsk Mountain Astronomical Station of the Pulkovo Observatory (STOP/KGAS). The study of variations of monthly indices and sunspot areas in the hemispheres revealed a pronounced asymmetry of sunspot formation during the period in favour of the southern hemisphere. It is shown that during the period under study, there was also a significant asymmetry both in the time of appearance of polar and low-latitude coronal holes and in their amplitude. At the initial stage, in the period from January 2020 to April 2022, the main contribution to the total area was made by polar coronal holes. Then, until the end of the period under consideration, low-latitude coronal holes, although at some points in time the contribution of both types of coronal holes was significant. A comparative analysis of the dynamics of the magnetic fluxes of coronal holes derived from the synoptic magnetic field maps of the HMI/SDO and STOP/KGAS instruments for the same period (2014–2024) showed good agreement between the results. This is a significant argument in favour of the regular use of domestic instruments, in particular STOP/KGAS, to study the evolution of the Sun's magnetic fields

Keywords: *Sun, solar activity, solar activity indices, solar cycle, magnetic fields, coronal holes*

DOI: 10.31857/S00167940250503e7

1. INTRODUCTION

Solar activity (SA) is a set of complex and interrelated phenomena initiated by the Sun's magnetic field [Vitinsky, 1983]. In each solar cycle, the magnetic field observed at the surface of the Sun exhibits an evolutionary pattern that is generally repeatable but unique in its details. Previously, the 11-year cycle was thought to be the most fundamental SA cycle [Nagovitsyn et al., 2015]. Currently, there is a paradigm shift in the concept of solar cycles. According to modern concepts, the physical and dominant cycle on the Sun is the 22-year magnetic solar cycle (SC]. This can be seen from a recent review [Martin, 2024]. There, it is also proposed to consider the 11-year cycle as the obligatory spot phase of any physical SO, when the pop-up magnetic fluxes reach the magnitude of spot formation. The different solar activity (Fig. 1) during the 11-year SO is formed by the interaction of magnetic fields of different characteristic scales. There are fields of relatively small scale (local), but they are quite strong, with strengths up to 3− 5 thousand Gauss, and form sunspots (SPs). The number of SPs varies during the cycle. At the beginning of the cycle they appear at high latitudes in small numbers, by the middle of the cycle (see Fig. 1, left) their number increases, and at the minimum they disappear (Fig. 1, right). But this does not mean that CA decreases at the same time as they do. In fact, it transitions into a phenomenon of a different characteristic scale. The Sun also has magnetic fields of lower strength on the order of hundreds of Gauss, but they cover a large part of the Sun's surface and change in antiphase with the local fields [Obridko & Nagovitsyn, 2017]. That is, when we see a minimum of SA by spots, we see a kind of maximum of SA by large-scale fields (in Fig. 1, right). One view is that the large-scale magnetic fields are a consequence of the decay of active regions and transport processes (see, e.g., [Yeates et al., 2023]).

Fig. 1.

Coronal holes (CHs) are local structures in unipolar regions of the large-scale magnetic field with open field lines that are the source of the solar wind [Abramenko et al., 2009; Cranmer, 2009; Obridko et al., 2009]. In them the strength is of the order of only a few Gauss. KDs have a reduced temperature and an anomalously low density [Priest, 2014]. The evolution of KDs is closely related to the evolution of the Sun's large-scale magnetic fields. Reorganizations of the global magnetic field and KD distribution occur simultaneously during a time interval of several solar revolutions [Bilenko and Tavastsherna, 2016]. By studying the dynamics of KDs, in particular their area, we can judge the dynamics of the Sun and how the cycle progresses. We can say that SP and CD are good indicators of SA throughout the cycle.

Two objectives were pursued in the course of the work. The first was to analyze the dynamics of some small-scale and large-scale solar formations - SP (a consequence of the development of the toroidal component of the Sun's total magnetic field) and KD (a consequence of the development of

the poloidal component**,** respectively) in the first five years of the 25th cycle, using variations of such SA indices as SP indices and areas, as well as areas and magnetic fluxes (MF) of KD. The second is to verify the obtained conclusions using several independent data sources.

2. CYCLE 25 AND SOLAR ACTIVITY INDICES

To describe the dynamics of 11-year solar activity cycles (Schwabe cycles− Wolf cycles), it is customary to use the smoothed cycle representation [Obridko, 2008]. According to the world network of solar activity level data (SILSO data/image, Royal Observatory of Belgium, Brussels), the values of monthly smoothed sunspot numbers reveal a minimum at the junction of 2019-2020. This allows us to consider that the 25th solar activity cycle began in January 2020 (https://www.sidc.be/SILSO/home). Solar Cycle (SC) 25 has already taken its place in the family of medium-large cycles, confirming once again that on the statistics of reliable (10-24) SCs within SA epochs, the observational rules and patterns of development of individual SCs are steadily fulfilled. The maximum point of the current SO with high probability will be passed by the end of 2024, with one peak, as well as all known reliable SOs of average magnitude, except for the transitional one between the epochs of SO23 [Ishkov, 2025]. The repolarization started from the northern hemisphere and took place rather quickly - from July 2023 to July 2024.

SA indices are numerical values describing its state at a particular point in time. Currently, there are a number of indices reflecting the measure of solar activity in its various manifestations. Some of them, the most famous, are presented on the website of the Kislovodsk Mountain Astronomical Station of the Main Astronomical Observatory of the Russian Academy of Sciences (GAAS GAO). These are the sunspot index, the Butterfly Maunder diagram reflecting the latitude-time dependence of the sunspot formation zone on the Sun, the area of sunspots, prominences, floccules, and coronal holes. The latter index reflects to some extent the magnitude of the magnetic flux through the surface of the Sun, concentrated in the above-mentioned formations. Many other different indices are also used. All of them give an idea of how solar radiation affects the Earth's magnetosphere.

2.1. Index of sunspots, SP and CD areas according to GAO GAS data in the 25th SA cycle

To analyze the SA in the first 5 years of cycle 25 (January 2020– January 2025), the paper considers variations in sunspot index, sunspot area, and coronal holes (Fig. 2). Data are taken from the Indexes section of the GAO GAS website (https://observethesun.com). The analysis of monthly values of the sunspot index and their areas (Fig. 2a*, b*) in hemispheres revealed a pronounced asymmetry of sunspot formation during this period in favor of the southern hemisphere. In the 25th cycle of monthly data for both hemispheres, the maximum value of the sunspot index reached 195.6,

and the maximum total area occupied by sunspots on 01.08.2024 amounted to 3753 TIR (millionths of a hemisphere).

Fig. 2.

During the study period, there was also a pronounced asymmetry in both the time of appearance of polar and low-latitude KDs and their amplitude (Fig. *2c*). At the initial stage, in the period from January 2020 to April 2022, the main contribution to the total area was made by polar KDs. Then, until the end of the period under consideration - low-latitude ones, although at certain moments the contribution of both types of CDs was significant. For example, the increase in the area of low-latitude CDs in March and June 2021 was reflected in the total area of the initial stage CDs. And starting from August 2024, the increase in polar KDs also contributed to the increase in the total area of KDs on the CA growth branch of Cycle 25. This result is consistent with the one we obtained earlier [Andreeva, 2024], for the areas of CDs extracted by the SPoCA (Spatial Possibilistic Clustering Algorithm) algorithm. Note, however, that we can judge the significance of the observed behavior of CDs in relation to the solar cycle only after observing the entire 25th cycle and in comparison with other cycles.

The paper further analyzes the variations of the magnetic fluxes of KD obtained from the observations of two instruments HMI/SDO [Scherrer et al., 2012] and STOP/GAS GAO [Peshcherov et al., 2013].

3. ANALYSIS OF THE DYNAMICS OF MAGNETIC FLUXES OF THE CD OBTAINED FROM THE HMI/SDO AND STOP/GAS GAO OBSERVATIONS

The input data for our work were synoptic maps (CK) constructed on the basis of observations with the AIA/SDO instrument [Lemen et al, 2012] at a wavelength of 193Å (see Fig. 3, upper panel, for an example of such a map), as well as CKs of the radial component of the magnetic field obtained with the HMI/SDO tool (maps hmi.mrsynop_small_720s from the site (http://jsoc.stanford.edu) without additional processing) and CKs of the magnetic fields of STOP/GAS GAO (Fig. 3, middle and lower panels, respectively). In the SC for Carrington Rotation (CR) 2259 (July 2022 - growth branch of CA cycle 25), the polar north, a small south and several low-latitude CRs are clearly visible. The construction of the AIA SCs and the selection of CDs on them was performed using the algorithms described in detail in [Illarionov and Tlatov, 2018; Illarionov et al., 2020]. Using this technique, we superimposed the KD contours identified from the AIA synoptic maps on the SCs of the HMI and STOP magnetic fields. As a result, we obtained variations of MF and areas of polar and low-latitude CDs for the entire observation period. For HMI, this is June 2010-October 2024, and for STOP, this is June 2014-November 2024. Next, we compared the MFs of the KDs obtained from the data of the two instruments over the same time interval: from June 2014 to December 2024 inclusive

(CR 2154– 2290). Figure 4 shows that the flows behave in a similar way. Note the slight dominance of the MF amplitude of polar KDs derived from HMI data (Fig. *4a*) at the minimum of CA 24/25 cycles. Conversely, for low-latitude KDs, there is an insignificant excess of the fluxes from the HMI data, especially at the beginning of the period under study (Fig. *4b*). We do not know yet how to explain this. But in general, we would like to note a rather good agreement of the obtained results.

Having such results, we considered the dynamics of the areas and MFs of polar and low-latitude CDs in the 25th SC in more detail - for the entire visible solar surface and separately in the N and S hemispheres.

Fig. 3.

Fig. 4.

3.1 Areas and magnetic fluxes of the visible solar surface KDs from AIA, HMI, and STOP data in the 25th CA cycle (CR 2226– 2290).

In Fig. 5 we present the areas (*a)* and total MFs of all CDs (*b*), as well as separately the fluxes of polar (*c*) and low-latitude (*d*) CDs of the visible solar surface for the two instruments. In Fig. 5 and Fig. 6, the gray line shows the fluxes derived from HMI/SDO observations, while the black line shows the fluxes derived from STOP/GAS GAO. It can be noted that all the MFs repeat the dynamics of the KD areas identified from the AIA/SDO SC. An asymmetry in the generation of polar and nonpolar KDs both in time and amplitude is observed.

In [Luhmann et al., 2022], an interpretation of the solar cycle trend is given. The appearance and development of different types of KDs are considered against the background of SP indices. The authors tell us that equatorial and low-latitude KD sources are present throughout the cycle and contribute to both the minimum and active phases of the solar cycle. At minimum, polar KDs are maximal, and during the growth phase, polar and midlatitude KDs come into play as new cycle active regions appear at their highest latitudes (≈ 35°) per cycle; during solar maximum, lower latitude sources again dominate, but favor locations off the equator where the most active late cycle regions appear. This trend is also seen in our results (see Fig. *5c– d*). The maximum of the polar CM flux occurs at the beginning of the 25th cycle, after which it begins to decrease markedly, and its value is minimal after February 2023. The main contribution to the total MF (Fig. *5b*) up to May 2022 is made by polar KDs, after which it is made by low-latitude KDs.

Fig. 5.

Fig. 6.

3.2 Magnetic fluxes of polar and low-latitude CDs in hemispheres from HMI and STOP data in the

25th CA cycle (CR 2226-2290)

Figure 6 shows the MF dynamics of KDs in the N- and S-semispheres during the study period. Polar (*a, c*) on the left and low-latitude (*b, d*) on the right. The observed hemispheric asymmetry of the MF of polar CDs is probably due to the variation of the inclination angle of the Sun's rotation axis (B_0) with time. The generation of polar CD MFs in the N hemisphere is pronounced until October 2022, then they practically disappear and resume in April 2024. In the S hemisphere, the MFs decrease from maximum to minimum values in April 2023, then they disappear and do not appear until the end of the period under study. In the 25th SA cycle, the MF generation of low-latitude CDs in the hemispheres occurs quasi-synchronously. The MF values of low-latitude CDs of the S hemisphere slightly exceeded the MF values of the N hemisphere.

4. CONCLUSION

The paper traces the dynamics of small- and large-scale solar formations - sunspots (a consequence of the development of the toroidal component of the Sun's total magnetic field) and coronal holes (a consequence of the development of the poloidal component) in the first five years of the 25th SA cycle.

The analysis of monthly values of the index and sunspot areas in hemispheres revealed a pronounced asymmetry of sunspot formation during this period in favor of the southern hemisphere.

For a more detailed study, the KDs were divided into polar and low-latitude ones and their behavior on the entire visible surface of the Sun, as well as in the northern and southern hemispheres, was considered. The paper shows that the areas and magnetic fluxes of polar CMs are maximal at the minimum and the beginning of the 25th solar cycle, then they begin to decrease and disappear during the SA growth phase. The main contribution to the total MF until May 2022 is made by the polar KDs, after that - by low-latitude KDs. There is a visible asymmetry between the north and the south both in the temporal behavior and in the magnitude of the areas and magnetic fluxes of CMs.

A comparative analysis of the dynamics of the magnetic fluxes of KD derived from the SC of magnetic fields observed by the HMI/SDO and STOP/GAS GAO instruments in the period from 2014 to 2024 showed a fairly good agreement. All the above conclusions on the magnetic fluxes of the KD are relevant for the data obtained by both instruments. This is a significant argument in favor of the regular use of domestic instruments, in particular the STOP/GAS GAO RAS telescope.

ACKNOWLEDGEMENTS

The authors are grateful to the SDO/HMI and GAS GAO/STOP teams for the opportunity to have access to observational data. The authors would like to thank A. G. Kosovichev for his help in

obtaining HMI/SDO synoptic magnetic field map data. We appreciate the efforts of the anonymous reviewers whose comments and criticisms led to the improvement of the manuscript.

FUNDING

This work was supported by the Ministry of Science and Higher Education of the Russian Federation under the State Assignment (Theme No. 122022400224-7).

CONFLICT OF INTERESTS

The authors declare that they have no conflict of interest with other researchers in the field.

REFERENCES

1. *Vitinsky Yu.I.* Solar activity. 2nd ed. Moscow: Nauka, 192 p. 1983.

2. *Ishkov V.N*. The current 25 solar cycle in the year of maximum: solar active phenomena and the forecast of their development on the branch of decline / Plasma physics in the Solar system / Collection of abstracts of the XX Annual Conference. Moscow, February 10-14, 2025. Moscow: IKI. P. 20. 2025.

3. *Obridko V.N*. Magnetic fields and activity indices / Plasma heliogeophysics. V. 1. Ed. by L.M. Zeleny, I.S. Veselovsky. M.: Fizmatlit. P. 41-59. 2008.

4. *Obridko V.N., Nagovitsyn Yu.A.* Solar activity, cyclicity and forecasting methods. St. Petersburg: VVM, 466 p. 2017.

5. *Caves V.S., Grigoriev V.M., Bevzov A.N. and others.* Solar telescope for operational forecasts of a new generation // Autometry. V. 49. No. 6. P. 62-69. 2013.

6. *Abramenko V., Yurchyshyn V., Watanabe H.* Parameters of the magnetic flux inside coronal holes // Solar Phys. V. 260. № 1. P. 43–57. 2009. https://doi.org/10.1007/s11207-009-9433-7

7. *Andreeva O.* Comparison of the dynamics of coronal holes identified by two detection methods in solar activity cycles 24–25 / Modern astronomy: from the Early Universe to exoplanets and black holes / Proc. All-Russian Astronomical Conference VAK-2024. Nizhny Arkhyz, August 25-31, 2024. P. 517–522. 2024. http://dx.doi.org/10.26119/VAK2024.097

8. *Bilenko I.A., Tavastsherna K.S.* Coronal hole and solar global magnetic field evolution in 1976–2012 // Solar Phys. V. 291. N 8. P. 2329–2352. 2016. https://doi.org/10.1007/s11207-016-0966-2

9. *Cranmer S.R.* Coronal holes // Living Rev. Sol. Phys. V. 6. ID 3. 2009. https://doi.org/10.12942/lrsp-2009-3

10. *Illarionov E.A., Tlatov A.G.* Segmentation of coronal holes in solar disk images with a convolutional neural network // Mon. Not. R. Astron. Soc. V. 481. № 4. P. 5014–5021. 2018.

https://doi.org/10.1093/mnras/sty2628
11. *Illarionov E.A., Kosovichev A.G., Tlatov A.G.* Machine-learning approach to identification of coronal holes in solar disk images and synoptic maps // Astrophys. J. V. 903. № 2. ID 115. 2020. https://doi.org/10.3847/1538-4357/abb94d
12. *Lemen J.R., Title A.M., Akin D.J. et al.* The Atmospheric Imaging Assembly (AIA) on the Solar Dynamics Observatory (SDO) // Solar Phys. V. 275. № 1–2. P.17–40. 2012. https://doi.org/10.1007/s11207-011-9776-8
13. *Luhmann J.G., Li Y., Lee C.O., Jian L.K., Arge C.N., Riley P.* Solar cycle variability in coronal holes and their effects on solar wind sources // Space Weather. V. 20. № 10. ID e2022SW003110. 2022. https://doi.org/10.1029/2022SW003110
14. *Martin S.* Observations key to understanding solar cycles: a review // Front. Astron. Space Sci. V. 10. ID 1177097. 2024. https://doi.org/10.3389/fspas.2023.1177097
15. *Nagovitsyn Yu.A., Georgieva K., Osipova A.A., Kuleshova A.I.* Eleven year cyclicity of the sun on the 2000-year time scale // Geomagn. Aeronomy. V. 55. № 8. P. 1081–1088. 2015. https://doi.org/10.1134/S001679321508023X
16. *Obridko V.N., Shelting B.D., Livshits I.M., Asgarov A.B.* Contrast of coronal holes and parameters of associated solar wind streams // Solar Phys. V. 260. № 1. P. 191–206. 2009. https://doi.org/10.1007/s11207-009-9435-5
17. *Priest E.* Magnetohydrodynamics of the Sun. Cambridge: Cambridge University Press, 580 p. 2014. https://doi.org/10.1017/CBO9781139020732
18. *Scherrer P.H., Schou J., Bush R.I. et al.* The Helioseismic and Magnetic Imager (HMI) investigation for the Solar Dynamics Observatory (SDO) // Solar Phys. V. 275. № 1–2. P. 207–227. 2012. https://doi.org/10.1007/s11207-011-9834-2
19. *Yeates A.R., Cheung M.C.M., Jiang J., Petrovay K., Wang Y.-M.* Surface flux transport on the Sun // Space Sci. Rev. V. 219. № 4. ID 31. 2023. https://doi.org/10.1007/s11214-023-00978-8

FIGURE CAPTIONS

Fig. 1. Images of the Sun obtained with the AIA/SDO instrument at line 193Å at the maximum (left) and minimum (right) of solar activity in cycle 24. The bright formations on the Sun's disk are active regions, the dark ones are coronal holes.

Fig. 2. Smoothed monthly solar activity indices of the 25th solar cycle from the GAO GAS data: (*a*) sunspot index, (*b*) sunspot areas, and (*c*) coronal holes over the entire visible surface of the Sun (dashed line), in the northern and southern hemispheres (gray and black lines, respectively).

Fig. 3. Example of a synoptic map derived from AIA/SDO observations at wavelength 193Å (upper panel) and CK magnetic fields from observations by the HMI/SDO and STOP/KGAS instruments (middle and lower panels, respectively) for the CR 2259 circulation. Latitude in degrees is plotted along the ordinate axis for the AIA CK, while the sine of latitude is plotted for the others. The contours indicate the boundaries of coronal holes.

Fig. 4. Magnetic fluxes of polar *(a)* and low-latitude *(b)* CMs of the visible solar surface derived from data of the HMI/SDO and STOP/GAS GAO instruments (solid and dashed curves, respectively) for the period 2014-2024.

Fig. 5. Areas and magnetic fluxes of coronal holes of the visible solar surface from AIA, HMI, and STOP data in the 25th SA cycle (CR 2226– 2290). (*a*) Total area calculated in % of sphere: dashed line is all, gray line is polar, and black line is low-latitude CDs. Total MFs of all (*b*), (*c*) polar and (*d*) low-latitude KDs. In panels (*b*– *d*), gray curves are fluxes derived from HMI/SDO observations, black curves are fluxes derived from GAO STOP/GAS observations.

Fig. 6. Magnetic fluxes of polar (*a, c*) and low-latitude (*b, d*) coronal holes in N- (*a, b*) and S- *(c, d*) hemispheres from HMI/SDO (gray curves) and GAO STOP/GAS data (black curves in solar cycle 25 (CR 2226– 2290).

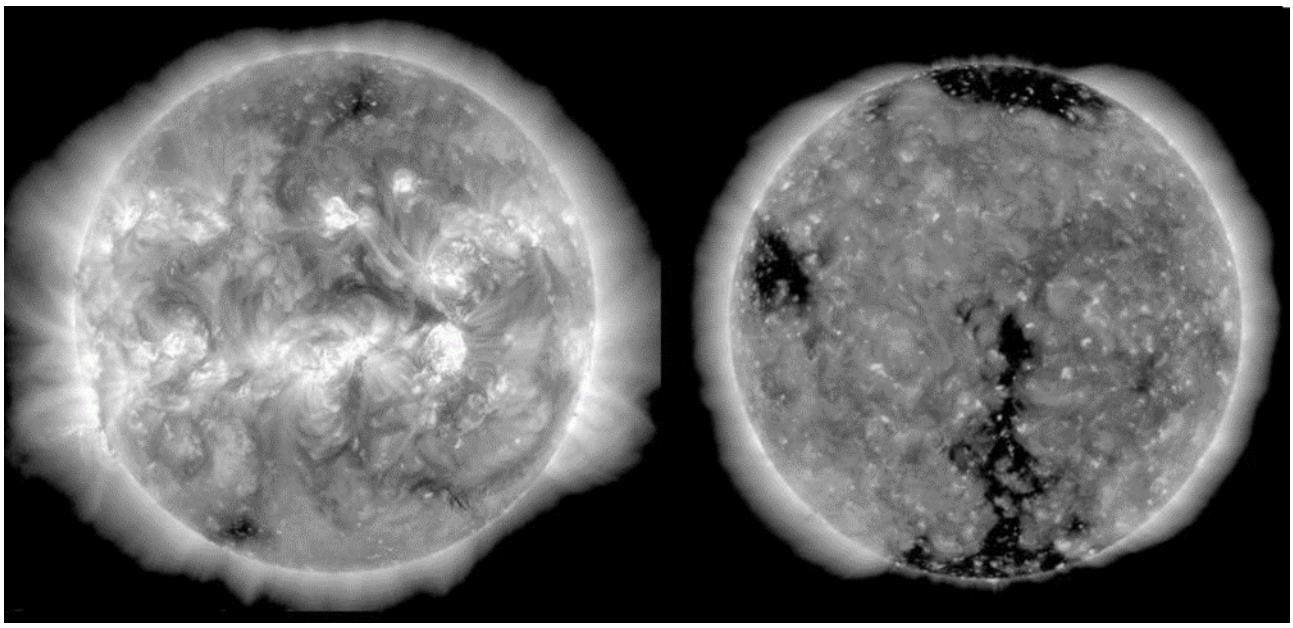

Fig. 1.

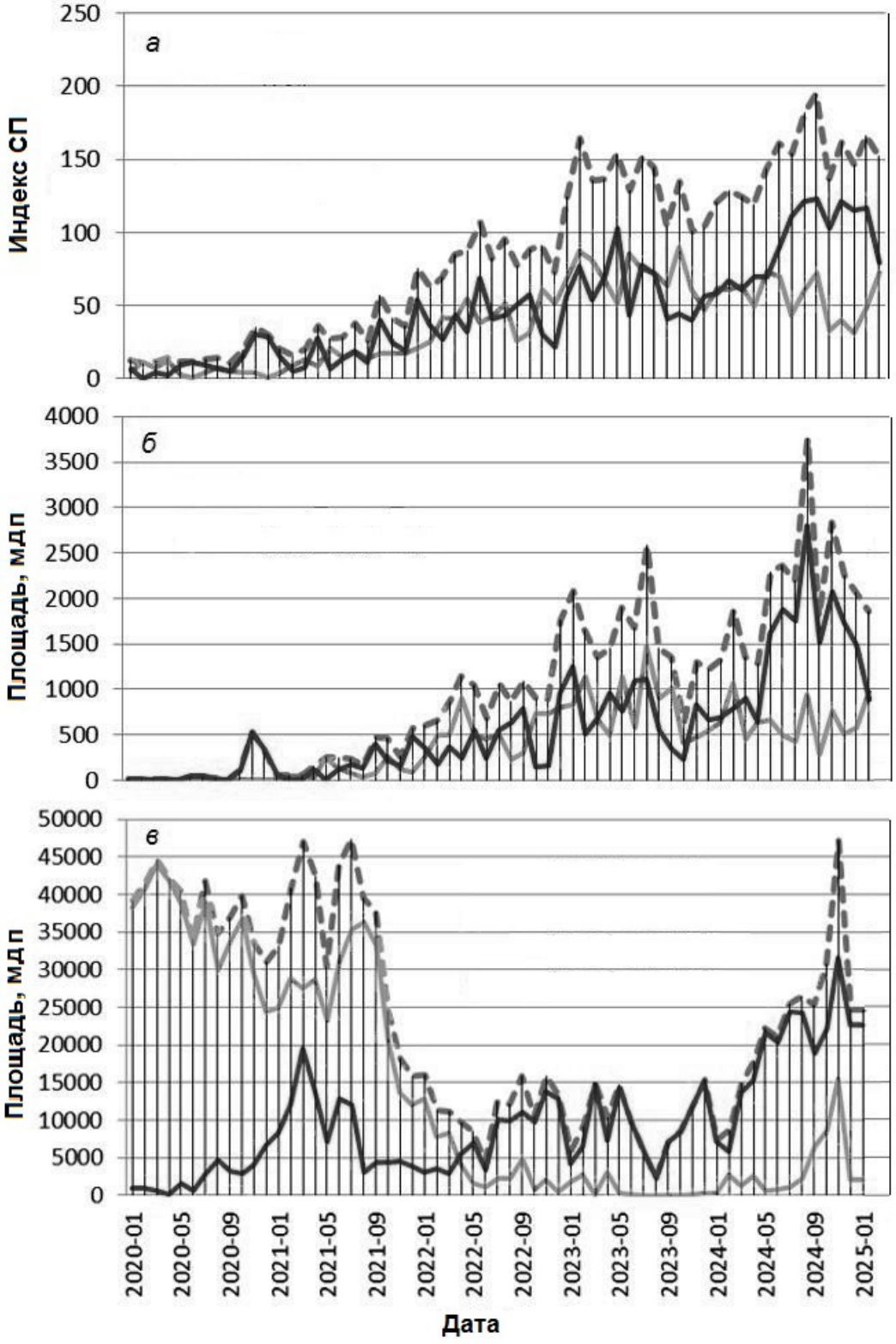
а
Индекс СП
250
200
150
100
50
0
б
Площадь, мдп
4000
3500
3000
2500
2000
1500
1000
500
0
в
Площадь, мдп
50000
45000
40000
35000
30000
25000
20000
15000
10000
5000
0
2020-01
2020-05
2020-09
2021-01
2021-05
2021-09
2022-01
2022-05
2022-09
2023-01
2023-05
2023-09
2024-01
2024-05
2024-09
2025-01
Дата

Fig. 2.

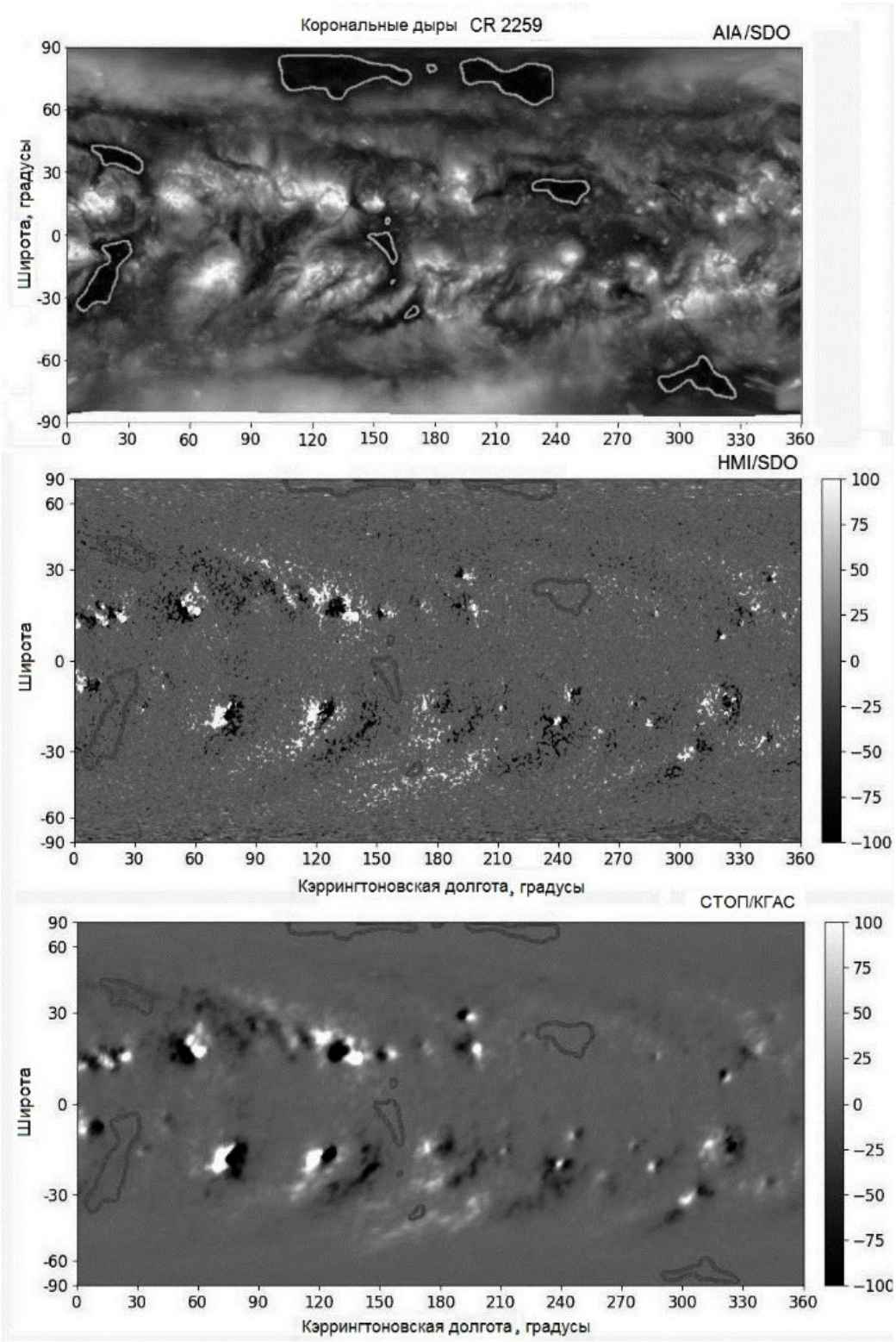
Корональные дыры CR 2259
AIA/SDO
Широта, градусы
HMI/SDO
Широта
Кэррингтоновская долгота, градусы
СТОП/КГАС
Широта
Кэррингтоновская долгота, градусы

Fig. 3.

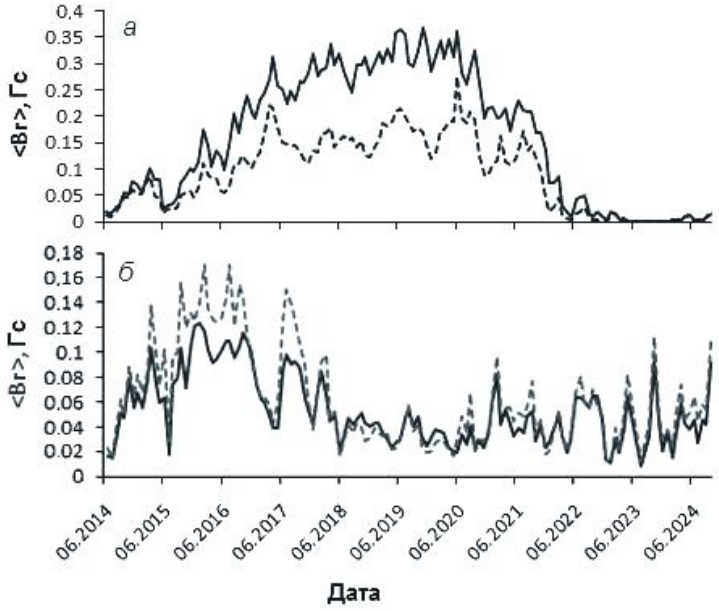

Fig. 4.

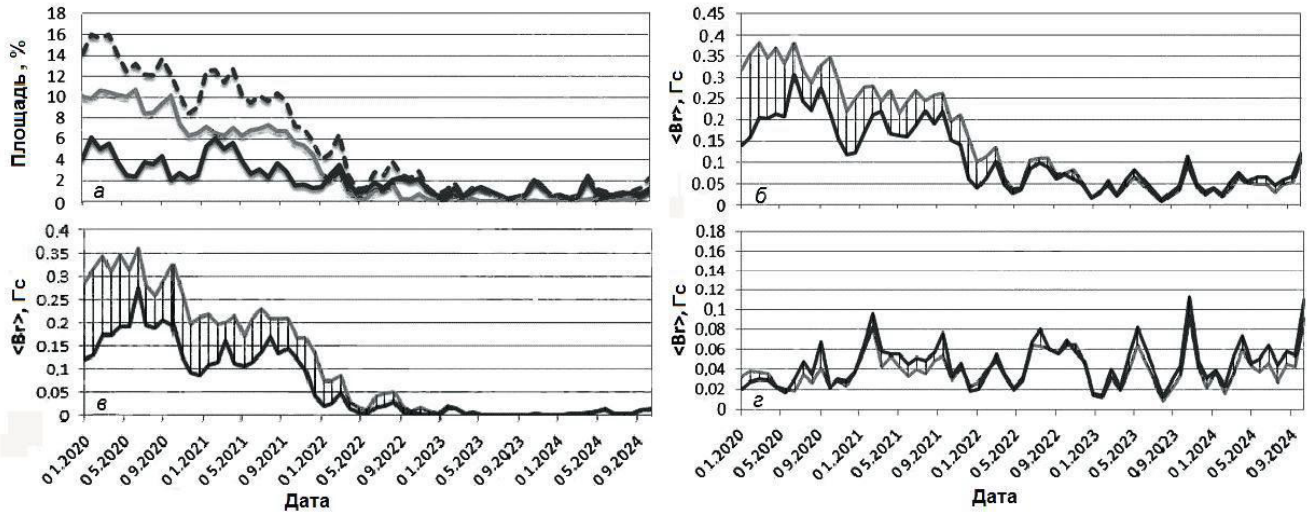

Fig. 5.

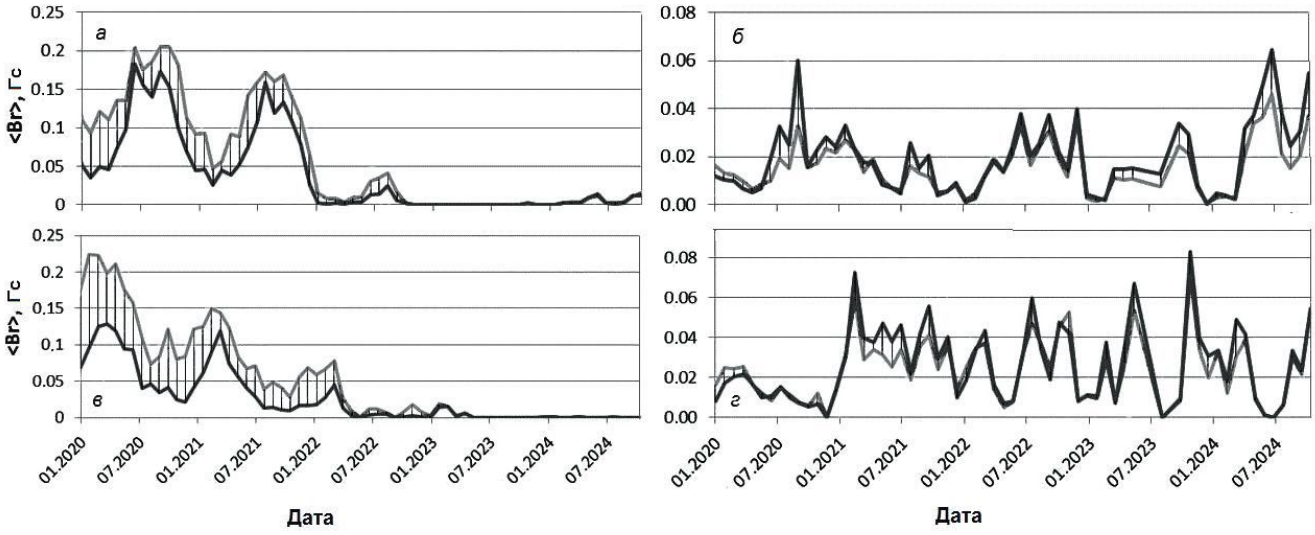
а
б
в
г

, Гс

, Гс
0.25
0.2
0.15
0.1
0.05
0
0.08
0.06
0.04
0.02
0.00
01.2020
07.2020
01.2021
07.2021
01.2022
07.2022
01.2023
07.2023
01.2024
07.2024
Дата
Дата

Fig. 6.